

25. L. S. Lebofsky, *Bull. Am. Astron. Soc.* **4**, 362 (1972).
26. H. C. Graboske, Jr., J. B. Pollack, A. S. Grossman, R. J. Olness, in preparation; J. B. Pollack and R. T. Reynolds, *Icarus* **21**, 248 (1974).
27. J. D. Anderson, G. W. Null, S. K. Wong, *Science* **183**, 322 (1974); in preparation.
28. B. Mason, *Space Sci. Rev.* **1**, 621 (1963).
29. J. S. Lewis has discussed the probable thermal history of icy objects, such as Ganymede [*Science* **172**, 1127 (1971); *Icarus* **15**, 174 (1971)]. On the basis of recent Pioneer 10 data, Anderson *et al.* (27) give a density of 3.5 g/cm³ for Io, which implies that Io, in bulk, is essentially free of H₂O ice. Therefore, if Io has a chondritic composition, as argued above, its postaccretion thermal history probably resembled those that have been calculated for a hypothetical initially cold and chondritic Earth moon [for example, see MacDonald, *J. Geophys. Res.* **64**, 1967 (1959)], which could allow extensive defluidization of Io. The density of Io is compatible with the densities of type III carbonaceous chondrites, which contain ~1 percent H₂O (28).
30. On the basis of the relationship between sublimation rates and temperatures given by K. Watson, B. C. Murray, H. Brown [*Icarus* **1**, 317 (1963)] and temperatures for Io's surface (1), about 2 km of H₂O ice could have sublimed from Io's surface in 4.5×10^9 years, so long as sublimation was the rate-limiting process. This might be so if the surface pressure was $\leq 10^{-11}$ bar. If the surface pressure is found to be as high as 10^{-8} bar (the Pioneer 10 upper limit) [A. Kliore, D. L. Cain, G. Fjeldbo, B. L. Seidel, S. I. Rasool, *Science* **183**, 323 (1974)], then ion production by megaelectron volt magnetospheric protons together with ion sweeping by the Jovian magnetosphere would cause the atmospheric mean residence time of H₂O ice to be on the order of ~4 years [Matson *et al.* (19)]. In the case of the "thick" atmosphere, up to a kilometer of ice could still be removed, since actual temperatures as high as 200 to 250 K may be inferred earlier in Io's history from the early luminosity history of Jupiter (26). These temperatures are above the H₂O ice-NH₃ ice eutectic (173 K).
31. This report presents the results of one phase of research carried out at the Jet Propulsion Laboratory, California Institute of Technology, under contract NAS 7-100, sponsored by the National Aeronautics and Space Administration. One of the authors (D.L.M.) was supported by a National Research Council resident research associateship during the period of this study. We thank J. S. Lewis, C. B. Pilcher, and D. B. Nash for helpful discussions.

29 April 1974; revised 15 July 1974

Modeling Periodically Surging Glaciers

Abstract. A numerical model has been developed which produces periodic surging as a characteristic of some glaciers for a certain accumulation and bed-rock distribution in contrast to the normal steady state for nonsurging glaciers. Results are presented to illustrate how the magnitude of changes in the length, thickness, and velocity of surging glaciers can be simulated by the model.

The sudden advance or "surge" of a glacier or ice cap after years of apparent stagnation or retreat remains one of the most fascinating and puzzling phenomena associated with these large ice masses. Such surges [in which the glacier moves forward often many kilometers over periods of months to years at speeds one or two orders of magnitude faster than normal (1)] occur in most glaciated regions of the world, and it has been suggested (2) that their occurrence in the Antarctic or Greenland ice sheets could have catastrophic consequences on a global scale (3).

Numerical models already developed for glaciers (4) give a reasonable approximation to their normal flow behavior but cannot be considered satisfactory unless they take into account the surging mode as well. Our aim in the work presented here was to develop a simple model which simulates the most important aspects of surging glaciers and which can be made more sophisticated to match their detailed features as further information on these becomes available. We present here preliminary results showing how the model reproduces various surge phenomena. The detailed theory of the

model and its application to specific surging glaciers will be described elsewhere (5).

For maximum simplicity we have used a two-dimensional model representing the central flow line of a glacier or a general flow line of an ice sheet. Techniques for determining the parameters of the central flow line for a given glacier have been described by Budd and Jenssen (4). The main principles upon which the surge model is constructed are as follows:

1) The average velocity V of a vertical ice column is composed of the average internal deformation through horizontal shear V_i plus the basal sliding velocity V_b :

$$V = V_i + V_b \quad (1)$$

2) One can obtain the average internal velocity of the column from the flow properties of the ice, for example, using a power law for flow

$$V_i = k \tau_b^n Z \quad (2)$$

where τ_b is the base stress, Z is the ice thickness, and k and n are flow law parameters of the ice.

3) The quantity V_b at a point is not directly related to other properties of the glacier at that point but is deter-

mined by the integral of the longitudinal strain rates along the glacier. This principle ensures that V_b and τ_b for the glacier as a whole are solved simultaneously to allow feedback and interaction so that their values at any one point interact with the values at other points.

4) The mean longitudinal strain rate through a column is governed by the equation of longitudinal stress equilibrium for scales large by comparison with Z and for small surface slopes α ($\sin \alpha \approx \alpha$) (6):

$$-2 \frac{\partial Z \bar{\sigma}_x'}{\partial x} = \tau_c - \tau_b \quad (3)$$

where $\bar{\sigma}_x'$ is the mean longitudinal stress deviator through the column at position x along the glacier and τ_c is the central downslope stress of the column given by

$$\tau_c = spg\alpha Z \quad (4)$$

where s is the shape factor for the glacier cross section (varying typically from 0.5 to 1 for symmetric shapes varying from semicircular to infinitely wide), ρ is the density of ice, and g is the gravitational acceleration.

Equation 3 expresses the large-scale balance between the three main forces on a longitudinal section element of the glacier, namely, the gravitational force downslope, the basal friction force of the bed upslope, and the difference between these forces over its ends.

5) The mean longitudinal strain rate through a column $\bar{\epsilon}_x$ is proportional to $\bar{\sigma}_x'$, that is

$$\bar{\epsilon}_x = \frac{\bar{\sigma}_x'}{2\eta} \quad (5)$$

Equation 5 provides for the extension or compression of the section of the glacier according to whether the longitudinal stress is greater or less than the overburden averaged through the thickness. The resultant strain rate is dependent on the flow properties of the ice.

For the simplest model we have taken the "generalized viscosity" η as a constant to show that a nonlinear flow law is not an essential requirement for surging. More general flow law relations can be used as required, such as a power law or a hyperbolic sine law. For development purposes Eqs. 2 and 5 allow the flow properties of the ice in horizontal shear and in longitudinal tension or compression to be studied independently. This is important for nonlinear flow laws for

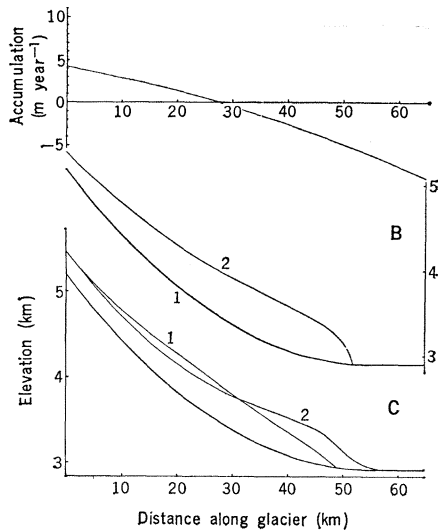


Fig. 1. (A) For the glacier model input the net accumulation-ablation balance rate a is shown as a function of distance along the glacier. (B) The bedrock elevation profile (curve 1) is shown as a function of distance together with the steady-state profile (curve 2) of a glacier resulting from the balance curve shown in (A). (C) For the surging model the glacier develops a periodically varying state in which the surface builds up slowly to a steep profile (curve 1), which rapidly changes to the extended flatter profile (curve 2) during the surge.

which the longitudinal stresses are not known.

6) Gross equilibrium of the whole glacier must be maintained; that is, if the value of τ_b is lowered in some part, it must increase correspondingly elsewhere. If the length of the glacier is L , then gross equilibrium over the whole glacier implies that

$$\int_0^L \tau_b dx = \int_0^L \rho g \alpha Z dx \quad (6)$$

7) The local τ_b at a point relative to the average τ_b is lowered according to the rate of production of water lubrication by the frictional energy dissipation of the sliding, $\tau_b V_b$, per unit area per unit time.

To provide for this in the simplest way possible we first introduce an expression which we call the "local relative lubrication-lowered stress" τ_c^* , first discussed by Budd and Radok (7) and defined by

$$\tau_c^* = \frac{\tau_c}{1 + \phi \tau_c V} \quad (7)$$

where the lubrication factor ϕ is a parameter which can be set as required but is ultimately determined through matching with real glaciers.

The quantity $\tau_b V_b$ could equally well

have been used here, but the total-motion energy dissipation $\tau_c V$ has been adopted instead because some contribution to the basal meltwater could perhaps come from melt produced by the internal deformation of the ice. However, since the production and flow of water in the ice mass is still not well understood, we will not dwell on this problem here except to say that the resultant differences to the model are small and primarily concealed in the numerical value of ϕ .

It is important to note that the expression τ_c^* alone cannot represent the local τ_b , because it allows only for stress lowering. If τ_b is lowered in some region, it must be increased elsewhere to preserve gross equilibrium. Hence from Eq. 7 and the condition of gross equilibrium we establish an expression for the local τ_b in terms of τ_c^* and averages over the length L , denoted by a bar, namely,

$$\tau_b - \bar{\tau}_b = \tau_c^* - \bar{\tau}_c^* \quad (8)$$

Many much more complex relations for τ_b could be used, but we consider Eqs. 7 and 8 to be the simplest relationships preserving gross equilibrium yet providing for a relative reduction of τ_b through frictional lubrication.

8) The variation of the glacier thickness with time is given by the equation of continuity for two dimensions as

$$\frac{\partial Z}{\partial t} = a - \frac{\partial VZ}{\partial x} \quad (9)$$

where a is the accumulation-ablation balance rate given as a function of x along the glacier.

The input to the computer program consists of the following: the glacier bedrock profile b and the accumulation-ablation balance a as functions of x (see Fig. 1); the ice flow law parameters k , n , and η ; and the frictional lubrication factor ϕ . As the glacier increases in size, both τ_b and V increase and so does the amount of sliding. If the value of $\phi \tau_b V$ remains small as the glacier nears its steady-state configuration, then the amount of sliding is also small and an ordinary steady-state glacier results. If the product $\phi \tau_b V$ becomes large before the steady state is reached, the sliding velocity increases giving rise to a further lowering of τ_b . This feedback creates the surge and the "fast mode" in which V is increasing while τ_b is decreasing. The high-velocity zone travels down the glacier to the front, causing the rapid advance.

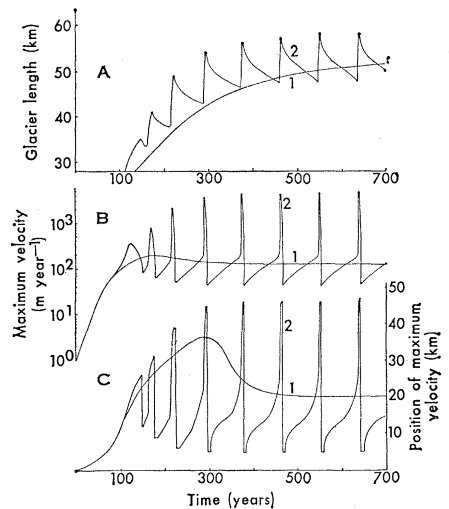


Fig. 2. The growth of the model toward steady state for an ordinary glacier (curve 1) and a surging type glacier (curve 2) is illustrated by the variation with time of the glaciers' length (A), the maximum velocity (B), and the position of the maximum velocity (C). The ordinary glacier gradually tends toward a constant steady state, whereas the surging glacier develops a periodically oscillating state characterized by a long period of slow buildup with retreat followed by a rapid advance at high speed. In the course of a surge cycle the position of maximum velocity travels down the glacier as a flux wave with increasing speed from the accumulation zone to the region of the terminus.

After this, the reduced τ_b from the reduced value of αZ brings the glacier back to the ordinary or "slow mode," and then the buildup starts again (see Fig. 1C).

We have carried out a large number of model calculations (~ 100), extending over the period from the initial development of a glacier to about 700 years by which time the final state of the glacier is apparent. Our object has been to study the scope of the model to simulate various features of real surges, for example, the duration of the surge; the period between surges; the magnitudes of advance and retreat; the maximum velocity of the surge; the critical values of V , V_b , and τ_b before the onset of the surge; and the effect of variations in the a and b curves.

Only a brief summary of the findings of these studies can be given here. Some results for one particular surge are illustrated in Fig. 2. The pattern of the surge cycle of the model has features similar to those described for real glaciers. After the surge the glacier is in a configuration with its terminus advanced beyond steady state and a lowered upper-accumulation zone, as

shown in Fig. 1C. The upper zone gradually builds up, and the advanced front ablates back. The zone of maximum velocity moves down from the upper region to the front as a wave (see Fig. 2C). The surge ends after this wave passes through the front of the glacier, and the position of the maximum velocity reverts to the upper region once more.

Onset of surge. For a given glacier (that is, for specified values of b and a) the onset of the surge depends on the values of ϕ and η . For a given η a certain critical value of ϕ separates surging from nonsurging conditions. Thus ϕ and η can be found to match real glaciers.

Size of the surge. The distance and speed of the surge can be increased by lowering η . From laboratory measurements of the flow law of ice it is apparent that realistic values of η will give rise to realistic values of surge speed and distance of advance. For greater sophistication, power law or hyperbolic sine functions could be used, but at this stage we are still attempting to find the appropriate order of magnitude.

Duration of the surge. The duration decreases as η decreases, when the ϕ value is set just above the critical value. Thus it is possible to vary the duration of the surge over a wide range. For the example chosen in Figs. 1 and 2 the change in length of 8 km occurs over 2 years.

Period of the surge. The main factors influencing the period of the surge cycle include the profiles of a and b , and the parameters ϕ and η . The length of the period is not simply related to the accumulation rate because it also depends on the magnitude of the surface lowering caused by the surge.

Shift of the equilibrium line. If a is changed to reduce the steady-state glacier size, a surging glacier can be changed to a nonsurging glacier that reaches a new steady state with a reduced length. Increasing the accumulation on a surging glacier increases the magnitude of the surge and also shortens its period.

Change in bedrock profile. A steeper bedrock gives rise to surges at lower ice thicknesses and lower velocities. For two glaciers that have the same curve of balance versus elevation, the steeper glacier will be shorter and thinner than the less steep glacier.

We believe that the simple program presented here can be used to match

real glacier surges to the first order of magnitude by suitable choice of the unknown parameters. Higher order approximations should be possible by refinements to the existing model. The matching of the model with real glaciers gives a method of determining the unknown parameters. We expect that the flow law and the lubrication functions eventually will be found to be general properties of ice and to be much the same for all temperate glaciers, with minor variations due to other influences such as bedrock properties and geothermal heat flux. The model developed here also provides a new way of treating the large-scale basal sliding of glaciers in which τ_b and V_b are not directly related at a point but are both determined instead by the properties of the whole glacier.

Finally, in our model no special physical conditions other than a and b distinguish surging from nonsurging glaciers. All glaciers are subject to the same laws. Some glaciers for their given situation reach the stage for which, through frictional lubrication, the basal sliding becomes dominant and the fast

mode sets in. For surging glaciers the accumulation cannot keep up the flow in the fast mode; thus the flow runs out and reverts to the low sliding or slow mode, and the glacier builds up once more.

W. F. BUDD

Antarctic Division,
Department of Science,
568 St. Kilda Road,
Melbourne, Victoria 3004, Australia

B. J. McINNES

Meteorology Department,
University of Melbourne,
Melbourne, Victoria 3052

References

1. M. F. Meier and A. Post, *Can. J. Earth Sci.* **6**, 807 (1969).
2. A. T. Wilson, *ibid.*, p. 911.
3. J. T. Hollin, *ibid.*, p. 903.
4. W. F. Budd and D. J. Jenson, in *Symposium on Snow and Ice in Mountain Regions* (General Assembly, Moscow, Aug. 1971), J. C. Rodda, Ed. (International Union of Geodesy and Geophysics—International Association of Hydrological Science Commission of Snow and Ice, Institute of Hydrology, Wallingford, Berkshire, England, in press).
5. W. F. Budd, *J. Glaciol.*, in press; B. J. McInnes, in preparation.
6. W. F. Budd, *J. Glaciol.* **9**, 19 (1970); *ibid.* **10**, 177 (1971).
7. ——— and U. Radok, *Rep. Progr. Phys.* **34**, 1 (1971).

27 November 1973; revised 26 February 1974 ■

Amorphous Solid Water: An X-ray Diffraction Study

Abstract. Water vapor that condenses on a metal surface at 10°K forms a non-crystalline phase of estimated density 1.2 grams per cubic centimeter. X-ray diffraction data of high precision and resolution have been analyzed to yield oxygen atom pair correlation functions. The positional correlation in amorphous solid water extends over only a few molecular radii, and the radial distribution of near-neighbor oxygen atoms in amorphous solid water is qualitatively different from that found in the low-pressure ice modifications. Amorphous solid water is a useful material for liquid water models because it can be studied under conditions such that the effects of static disorder and thermal excitation can be separated.

Despite intensive study for many years, our understanding of the properties of water is primitive. Two factors have contributed heavily to the difficulties encountered. First, water is a polyatomic fluid with strong directional molecular interactions. The available statistical mechanical theories of the liquid state are inadequate for the description of water, and thus theory has not been of much use as a guide to experiment. Second, in the normal condition, at room temperature and atmospheric pressure, positional and orientational disorder in water are hopelessly intermixed with the effects of thermal excitations; hence experimental studies have not yet made it possible to separate the roles of static

disorder and dynamical disorder and have been inadequate to guide the development of a theory of the properties of the liquid.

In view of the situation described, Olander and Rice (1) sought for a model of water that could be studied under conditions such that the effects of static disorder and thermal excitation could be separated. They suggested that amorphous solid water might be such a model material.

Amorphous solid water was first reported by Burton and Oliver (2) in 1935, and a few studies of this material have been reported during the succeeding four decades (3). In most of these studies the solid was produced by the condensation of water vapor on